Available online at:
http://journal.unila.ac.id/index.php/tropicalsoil
DOI: 10.5400/jts.2023.v28i1.31-38

An Analyze of Urban Temperature Using Energy Balance Algorithm for Land (SEBAL) in Yogyakarta City

Nursida Arif[1*] and Nasir Nayan[2]

[1]*Department of Geography Education, Faculty of Social Science, Universitas Negeri Yogyakarta , Indonesia*
[2]*Jabatan Geografi dan Alam Sekitar, Fakulti Sains Kemanusiaan, Universiti Pendidikan Sultan Idris, Malaysia*
e-mail: nursida.arif@uny.ac.id

Received 30 April 2022, Revised 18 August 2022; Accepted 20 September 2022

ABSTRACT

This study aims to assess the level of disaster vulnerability in the Wonolelo Tourist Village by applying spatial analysis through an overlay method that integrates multiple contributing factors to disaster risk. Located on the slopes of Mount Merapi, Wonolelo Village features moderately steep to steep topography, making it particularly susceptible to both volcanic eruptions and landslides. The spatial analysis results indicate that Wonolelo Village has a high vulnerability to volcanic disasters (63.71%) and a moderate vulnerability to landslides (99.12%). These findings highlight the urgent need for comprehensive and location-specific disaster risk reduction strategies, especially in areas with similar geological and topographical conditions. This research contributes to the field of disaster risk management by offering a spatially driven vulnerability assessment framework that can inform the development of early warning systems, land-use planning, and targeted mitigation policies not only for Wonolelo Village but also for other high-risk tourist and rural regions situated in disaster-prone zones.

Keywords: Land surface temperature, SEBAL, Yogyakarta

INTRODUCTION

The density of the urban population contributes to climate change due to pressure on land use (Ilcheva and Yordanova 2019). The advantages of the city as a center of economic activity encourage the acceleration of urbanization, which impacts the complexity of problems in the city (Arif et al. 2019; Chrysoulakis et al. 2018). Conversion of land from non-built into built-up land results in increased air temperature reduces evapotranspiration and causes drought (Tursilowati et al. 2012). On the other hand, if the vegetation cover increases, the temperature will decrease (Goward et al. 2002). The vegetation dynamics are significantly influenced by geographical factors, climate, and the inhabitants' everyday activities (Kalisa et al. 2019). The importance of vegetation land cover in sustaining the urban climatic balance cannot be overstated. As a result, cities with dense populations must factor green space availability into urban design and development.

This study focuses on land surface temperature (LST) in Yogyakarta's various land cover/land use (LULC) categories. Yogyakarta city is an essential part of the Yogyakarta Special Region's development as an Indonesian province since it is one of the most important centers of education and tourism domestically and internationally (Cahya et al. 2017). This fact has allowed the city to grow by expanding the number of built-up areas, such as student boarding houses, apartments, and hotels. This study combined remote sensing technology and geographic information system (GIS). At the micro to macro scale, remote sensing has the advantage of consistency of observation and up-to-date spectral reflectance and land surface radiation (Bastiaanssen et al. 1998a). Remote sensing and geographic information systems (GIS) are essential tools in a range of applications related to this topic, including the study of urban climates (Nwaerema et al. 2019; Pal and Ziaul 2017), fractional vegetation cover mapping (Arif et al. 2020; Timmermans et al. 2007), LST mapping (Arif et al. 2019; Weng 2009), green space area (Chan and Vu 2017; Oliveira et al. 2011) and thermal monitoring city (Zhou et al. 2019; Zinzi and Carnielo 2017).

Land Surface Temperature is essential in urban energy studies and climatology (Khandelwal et al. 2018). LST is used to measure the temperature of

the city's surface heat because it takes into account the radiation of the earth's surface (Pal and Ziaul 2017). The characteristics of LULC are closely related to LST (Weng 2009). The temperature characteristics of various types of LULC are investigated in this study on two separate days, namely the rainy day and the dry day. Previous studies have shown a relation between LST and LULC, with vegetation land cover having a lower surface temperature than built-up areas (Weng 2009). The Surface Energy Balance Algorithm for Land (SEBAL) method examined LST. The main objective of SEBAL modeling was to determine how the visible and thermal infrared channels of different surface types, such as dry land and wetlands, interacted (Bastiaanssen et al. 1998a; Bastiaanssen et al. 1998b). By analyzing the effects of vegetation and soil, the SEBAL model can accurately estimate land surface temperature (Song et al. 2016). The objective of the vegetation index analysis was to examine the properties of the vegetation both geographically and temporally. SEBAL estimates canopy radiation as a function of NDVI using a semi-empirical method (Rahimzadegan and Janani 2019; Timmermans et al. 2007). The weighted difference vegetation index (WDVI) and the soil-adjusted vegetation index (SAVI) are two more approaches to estimating the vegetation index that can be utilized in the SEBAL calculation (Clevers 1991). The soil aspect is highlighted using SAVI (Huete 1988). The SEBAL model's different vegetation index formulas are expected to improve accuracy and decrease LST information. Land surface temperature mapping greatly benefits city planners in developing policy designs considering environmental conditions, climate, and citizens' comfort.

MATERIALS AND METHODS

Study Area

The city of Yogyakarta, which is located at 7°48'5" N and 110°21'52" E, is the case study for this study (Figure 1). Yogyakarta is the seat of the Yogyakarta Special Region, one of Indonesia's provinces. Yogyakarta has a tropical monsoon climate, with precipitation below 60 millimeters in August, the driest month.

Data Collection

The USGS Global Visualization Viewer provided the Landsat 8 OLI imagery utilized in this inquiry. The Landsat imaging records the earth's surface every 16 days, allowing for regular monitoring of a given area. Each Landsat pixel has a geographical coverage of 30 m and a radiometric resolution of 12

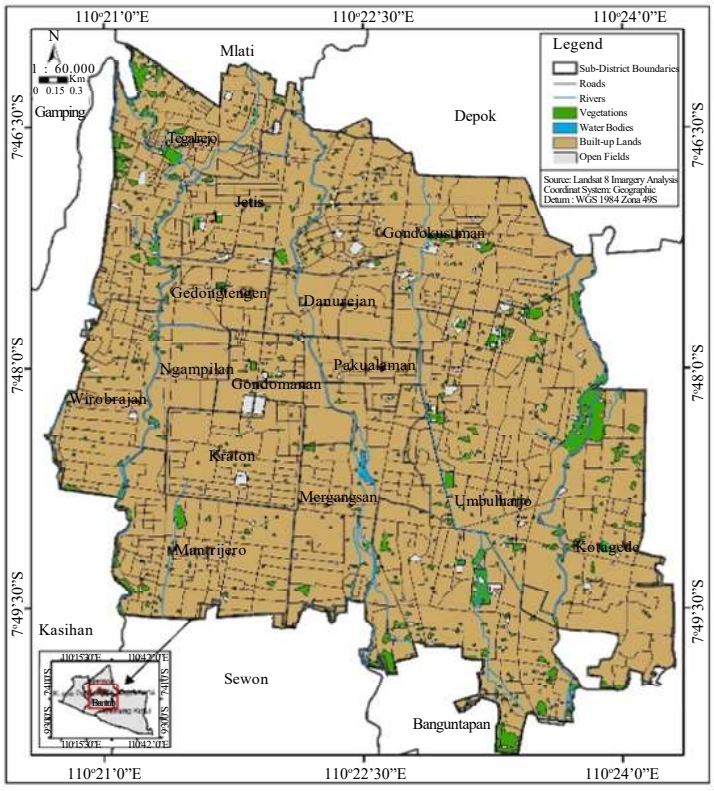

Figure 1. The LULC map of Yogyakarta City.

Table 1. Image data source.

	Data acquisition
Landsat 8 wet day	22 April 2019
Landsat 8 dry day	25 June 2019

(http://earthexplorer.usgs.gov 2019)

bits. Table 1 shows the Landsat 8 data that were used in this investigation.

Surface Energy Balance Algorithm for Land

In this study, the SEBAL algorithm was used to estimate land surface temperature, and this model uses near-infrared sensors and thermal infrared in Landsat imagery. British et al. (2002) arrange the stages used in SEBAL as follows.

(1). Convert Digital Number (DN) values to radians for thermal bands (bands 10 and bands 11) using the band math according to the following formula:

$$L\lambda = MLQcal + AL$$

Where,
Lλ = spectral radians on the sensor (W / (m2sr. Ìm)
Qcal = pixel value (DN)
ML = rescaling constant (RADIANCE_ MULT_ BAND_x, where x is the band used)
AL = constant (RADIANCE_ADD_BAND_x, where x is the band used

(2). Convert DN values to reflectance for non-thermal bands according to the following formula:

$$\rho\lambda' = M\rho Qcal + A\rho$$

where,
ρλ‘= Image reflectance values (min and max values are listed in the image header)
Qcal = pixel value (DN),
Mρ = rescaling constant (REFLECTANCE_ MULT_BAND_x, where x is the band used)
Aρ = adder constants (REFLECTANCE_ ADD_ BAND_x, where x is the band used)

(3). The reflectance value (ρλ’) has not been corrected with d = the sun’s angle. To get the TOA reflectance value, we need to correct the sun’s angle with the equation:

$$\rho\lambda = \frac{\rho\lambda'}{cos(\theta sz)} = \frac{\rho\lambda'}{sin(\theta se)}$$

Where,
ρλ = TOA planetary reflectance (without units),
ρλ‘= previous processing results, without correction of the taking angle
θSE = Sun elevation angle when recording (sun elevation) obtained in the image header
θSZ = zenith angle; θSZ = 90° - θSE αtoa

(4). Calculating the value of Albedo. Surface albedo is the ratio of the sun’s electromagnetic radiation reflected from the surface of the soil and plants to the incoming radiation (Song et al. 2019). Albedo is calculated from the following equation.

$$\propto = \frac{\propto_{toa} - \propto_{path-radiance}}{\tau sw^2}$$

$$\propto_{toa} = \sum(\omega\lambda\, x\, \rho\, \lambda)$$

$$\omega\lambda = \frac{ESUN_\lambda}{\sum ESUN_\lambda}$$

$$\tau sw^2 = 0.75 + 2\, x10^{-5} x\, z$$

where,
α = Albedo, the ratio between the rays of the sun that arrives at the surface of the earth and that is reflected into space
$\propto_{toa}$ = Albedo on the surface of the atmosphere (Albedo at the top of the atmosphere)
$\propto_{path-radiance}$ = albedo path radiance
ρ λ = reflectivity for band λ
τsw = shortwave transmissivity of air
ωλ = weighting coefficient for band λ

(5). Calculate NDVI values with the formula:

$$NDVI = \frac{\alpha NIR - \alpha RED}{\alpha NIR + \alpha RED}$$

where,
NDVI = NDVI value
αNIR = reflectance at near long-wavelength (band 5)
αRED = reflectance at the length of the infrared band (band 4)

(6). Calculates the *Weighted Life Vegetation Index* (WDVI) value according to the following formula

$$WDVI = NIR - \alpha RED$$

where,
WDVI = WDVI value
NIR = near-infrared band (band 5)
α = coefficient equation of the relationship of the infrared band close to the infrared band
RED = infrared band (band 4)

(7). Calculating the Soil Adjusted Vegetation Index (SAVI) value using the equation:

$$SAVI = \left(\frac{(NIR - RED)(1 + L)}{(NIR + RED + L)}\right)$$

where,
SAVI = SAVI value
NIR = near-infrared band
RED = infrared band
L = Monin-Obukhuv length
L = 1 - 2 × a × NDVI × WDVI, a = 1.6

(8). Calculate LAI values using equations

$$LAI = \left(\frac{\ln\left(\frac{0.69 - SAVI}{0.59}\right)}{0.91} \right)$$

In practice, the LAI value used is adjusted to the following conditions.
LAI = 11 * SAVI ^ 3 (for SAVI ≤ 0.817), or
LAI = 6 (for SAVI> 0.817)

(9). Calculates the object's emissivity value
εNB = 0.97 + 0.0033 * LAI; (for LAI <3)
ε0 = 0.97 + 0.0033 * LAI; (for LAI <3)
εNB = 0.98 and ε0 = 0.98 when LAI ≥ 3
where,
- the εNB value is used in the calculation of surface temperature
- the value of ε0 is used to calculate the total longwave radiation emission from the surface

(10). Calculates the corrected thermal radians (Rc)

$$Rc = \frac{L6 - Rp}{\tau NB} - (1 - \varepsilon NB)Rsky$$

where,
L6 = spectral radians of band 6 corrected
Rp = path radians
Rsky = thermal radiation in a narrow band when the sky is clear
τNB = air transmission in narrowband

(11).Calculate surface temperature (Ts)

$$Ts = \frac{K2}{\ln\left(\frac{\varepsilon NB\ K1}{Rc} + 1\right)}$$

where,
Ts = surface temperature (K)
K1, K2 = constants from Landsat images
Rc = corrected thermal radians value

In the process, the surface temperature calculation is used for each thermal band, namely band 10 and band 11. Then, the value of the surface temperature is actually calculated, i.e., the average value. Next, a calculation is performed to get the temperature value to Celcius (Celcius = Kelvin - 273.15)

Tskelvin = (TsB10 + TsB11) / 2; (Ts in Kelvin)
Tscelcius = Ts in Kelvin-273.15; (Ts in Celsius)

RESULTS AND DISCUSSION

Supervised classification divides pixels into land cover classes based on their pixel values' similarity to the region of interest (ROI). Land cover classification is carried out using the maximum likelihood classification because it shows better results than the unsupervised classification, where several classes are automatically entered, which can lead to possible errors in classification (Gadrani et al. 2018). In the earlier studies, LULC was applied to determine the relationship with LST (Arif et al. 2017; Guha and Govil 2020; Pal and Ziaul 2017; Weng 2009; Weng and Lu 2008). The built-up area takes up 94.19 percent of the total area on the LULC map, while the non-built-up area takes up the rest (vegetation, open land, water body). Yogyakarta is thus a densely populated city with a varied range of functions. Table 2 shows the percentages of each LULC.

Table 3 shows that the higher temperature in the image recorded on a dry day is 35.17°C compared to the image recorded on a wet day, with the highest temperature being 32.11°C. Figure 2 shows the results of the spatial distribution of LST on two different days. The Kraton, Gondomanan, Pakualaman, Danurejan, Jetis, Mergangsan, Gondokusuman, Ngampilan, Wirobrajan, and part of the Kotagede districts have maximum dry day temperatures in the range of 31-33°C. The Tegalrejo districts and Umbulharjo have the highest temperatures, with temperatures ranging from 29 to 31°C. Correlation between LST and ground truth is presented in Figure 3.

Figure 3 shows a high correlation between LST values and ground truth with an R-value of 0.64.

Table 2. LULC area.

LULC	Area (%)
Open field	1.88
Waterbody	0.08
Buil up area	94.19
Vegetation	3.86

(analysis 2020)

Table 3. LST value of study area.

	Wet day (°C)	Dry day (°C)
Average	26.79	30
Maximum	32.11	35.17
Minimum	13.63	25.24
Standard deviation	2.44	1.35

(analysis 2020)

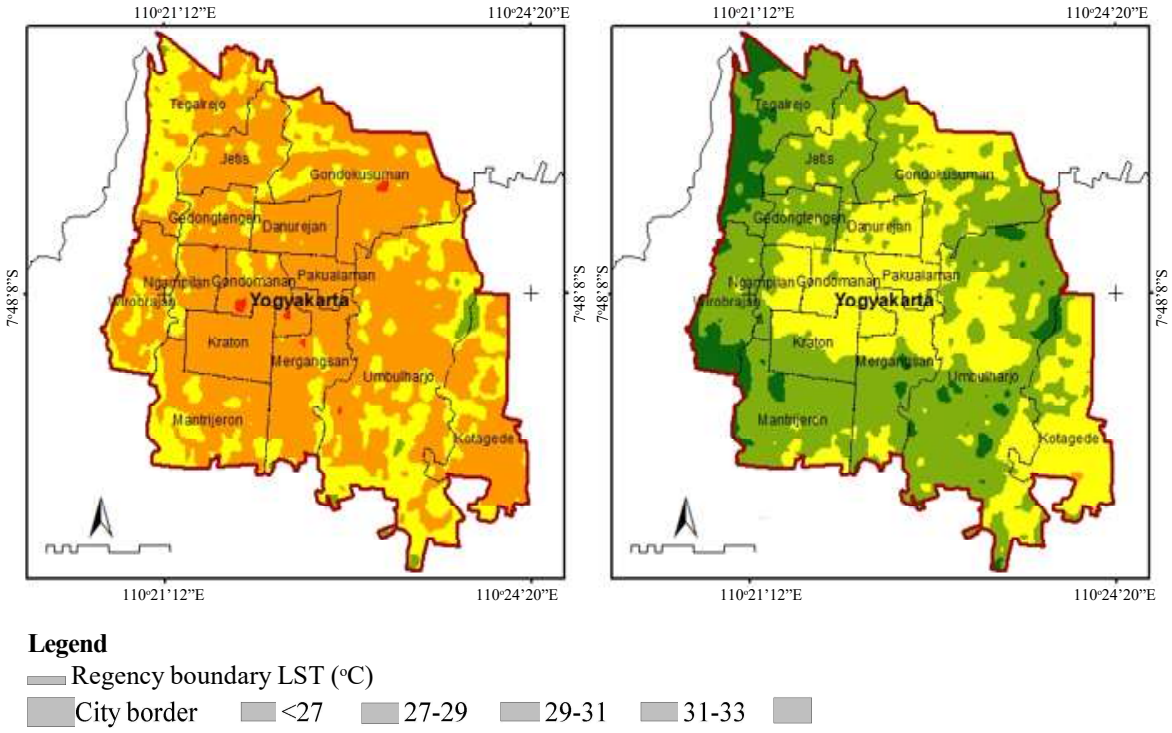

Figure 2. a). The LST on a dry day; b) The LST map on the wet day (analysis 2020).

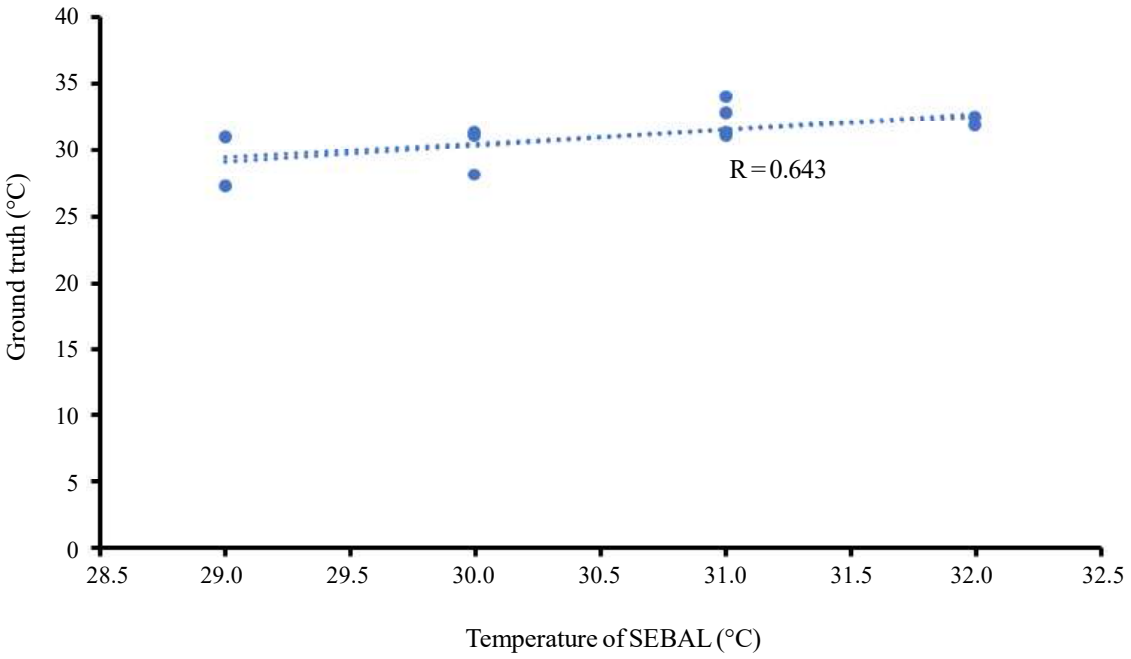

Figure 3. LST and ground truth correlation (analysis 2020).

Gondomanan, Pakualaman, Danurejan, part of Gondokusuman, Kotagede, region of Kraton, and Mergangsan have high temperatures in the 29-31°C range on rainy days. In the Kotagede district, temperatures in the 31-33°C range are only observed in a small area. On a dry day, LST with a temperature range of 33-35°C can be found in some regions, but not on a rainy day. The highest LST pattern was clustered in the city center, precisely in Danurejan, Gondomanan, and Pakualaman districts, as in Sumunar et al. (2020), with the highest LST pattern, was found in the city center, particularly in Danurejan, Gondomanan, and Pakualaman districts. Sumunar et al. (2020) stated that the land surface

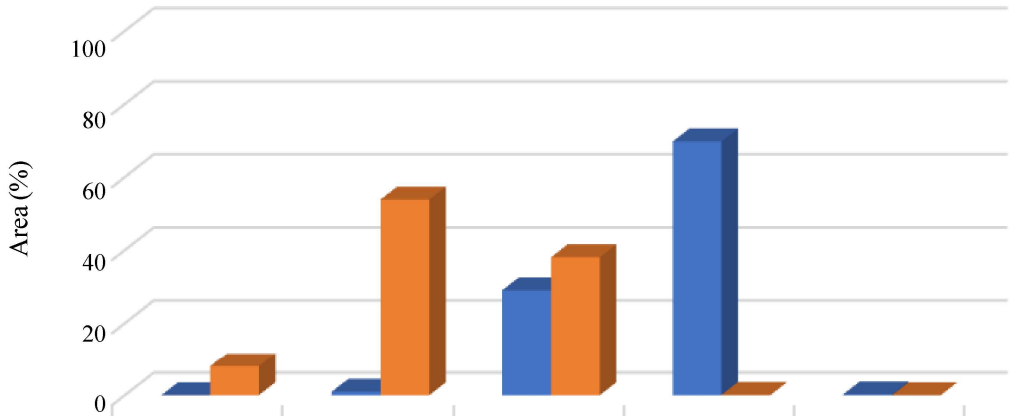

	23 - 27	27 - 29	29 - 31	31 - 33	33 - 35
Dry day (%)	0.00	0.98	29.00	69.75	0.26
Wet day (%)	8.02	53.85	38.05	0.09	0.00

Figure 4. Graphic percentage distribution of LST on a dry day and the wet day (analysis 2020)

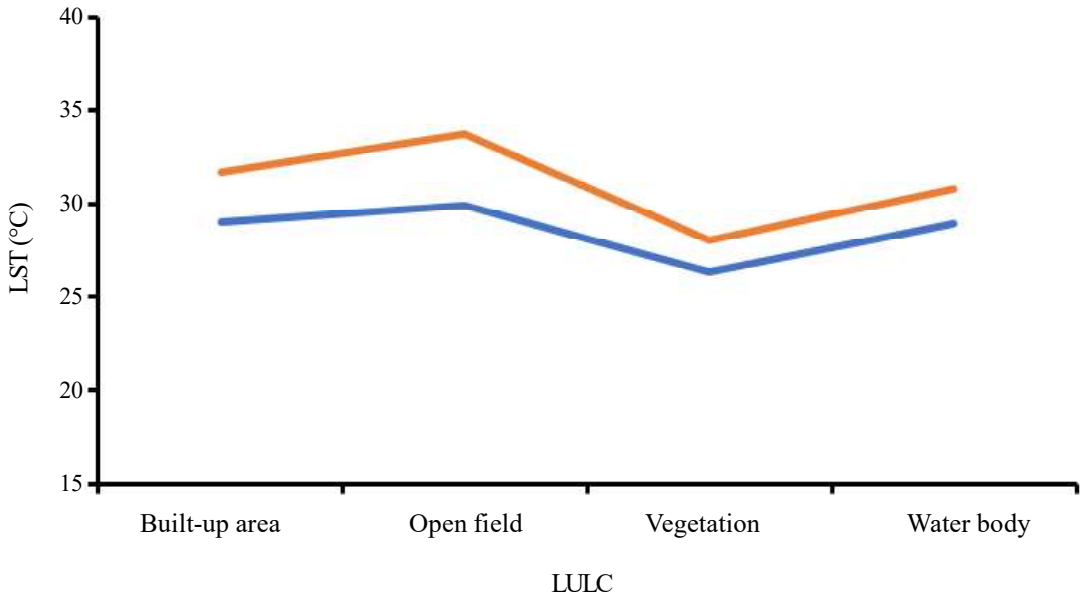

Figure 5. LST values for various LULC types. : LST wet day, : LST dry day.

temperature in Yogyakarta is clustered in the same area where the area is the center of economic activity with the dominance of built-in land, namely the Danurejan district and its surround. The following Figure 4 shows the details of each temperature range's area.

On a dry day, the highest temperature range is 33-35°C, which is spread over 0.26 percent of the whole area, while the minimum temperature range is 27-29°C, which is distributed in roughly 0.98 percent of the total area, as shown in Figure 4. On a wet day, the maximum temperature range of 31-33°C is found in only 0.09 percent of the whole area, but the maximum temperature range of 27-29°C is found in 53.85 percent. Many factors influence the difference in surface temperature, including city surface roughness (Burakowski et al. 2018), the thermal properties of the city's surface objects, which vary depending on their position and orientation in the form of roof and wall qualities (Voogt and Oke 2003), and the biophysical conditions of the soil (Weng 2009). Figure 5 shows the impact of land use on LST values in this study.

Figure 6 illustrates a similar pattern, namely that the temperature of the vegetation is lower than that of open land and built-up areas. This study's

SEBAL processing shows that vegetation causes a low land surface temperature (Khandelwal et al. 2018). Green spaces are essential in urban areas because they create a cooling effect (Oliveira et al. 2011). As a result, based on Yogyakarta's predominant land use, urban planners should consider expanding the green space area.

CONCLUSIONS

The SEBAL approach, which combines remote sensing and GIS, helps map urban land surface temperatures. The results of LST mapping show that the average temperature in the wet day recording image is 26.79°C. While the average temperature on a dry day recorded images are 30°C. The LST value is correlated with LULC, where high temperatures are distributed in open land and built-up land, and lower temperatures are found in vegetation land cover. High LST values are clustered in several sub-districts around the city center, namely Gondomanan, Danurejan, Pakualaman, and surrounding districts.

ACKNOWLEDGMENTS

The authors would like to thank Yogyakarta State University's Institute of Research and Community Service (LPPM) for their financial support of this study.

REFERENCES

Arif N, P Danoedoro and Hartono. 2017. Analysis of artificial neural network in erosion modeling: a case study of Serang Watershed. *IOP Conference Series: Earth and Environmental Science* 98: 012027. doi: https://doi.org/10.1088/1755-1315/98/1/012027.

Arif N, P Danoedoro, Hartono and A Mulabbi. 2020. Erosion prediction model using fractional vegetation cover. *Indonesian J Sci Tech* 5: 125-132. doi: https://doi.org/10.17509/ijost.v5i1.21060.

Arif N, AN Khasanah, R Jaya, M Gozan and B Hendrawan. 2019. The effect of land surface temperature and land use on energy system development in Gorontalo City. *J Phys: Conf Ser* 1179: 012103. doi: https://doi.org/10.1088/1742-6596/1179/1/012103.

Bastiaanssen WGM, M Menenti, RA Feddes and AAM Holtslag. 1998a. 1 A remote sensing surface energy balance algorithm for land (SEBAL). 1. Formulation. *J Hydrology* 213: 198-212.

Bastiaanssen WGM, H Pelgrum, J Wang, Y Ma and JF Moreno. 1998b. A remote sensing surface energy balance algorithm for land (SEBAL).: Part 2: Validation. *J Hydrology* 212: 213-229.

British N, R Waters, R Allen, M Tasumi, R Trezza and W Bastiaanssen. 2002. *SEBAL,* surface energy balance algorithms for land. Advance training and users manual. Idaho: a NASA EOSDIS/Synergy grant from the Raytheon Company University of Idaho, pp 1-97.

Burakowski E, A Tawfik, A Ouimette, L Lepine, K Novick, S Ollinger, C Zarzycki and G Bonan. 2018. The role of surface roughness, Albedo, and Bowen ratio on ecosystem energy balance in the Eastern United States. *Agr Forest Meteorol* 249: 367-376. doi: https://doi.org/10.1016/j.agrformet.2017.11.030.

Cahya GA, YKD Mahendra and II Damanik. 2017. Malioboro as a value of Special District of Yogyakarta City. *IOP Conference Series: Earth and Environmental Science* 70: 012055. doi: https://doi.org/10.1088/1755-1315/70/1/012055.

Chan KM and TT Vu. 2017. A landscape ecological perspective of the impacts of urbanization on urban green spaces in the Klang Valley. *Appl Geogr* 85: 89-100. doi: https://doi.org/10.1016/j.apgeog.2017.06.002.

Chrysoulakis N, S Grimmond, C Feigenwinter, F Lindberg, JP Gastellu-Etchegorry, M Marconcini, Z Mitraka, S Stagakis, B Crawford, F Olofson, L Landier, W Morrison and E Parlow. 2018. Urban energy exchanges monitoring from space. *Scientific Reports* 8: 1-8. doi: https://doi.org/10.1038/s41598-018-29873-x.

Clevers JGPW. 1991. Application of the WDVI in estimating LAI at the generative stage of barley. *ISPRS J Photogramm* 46: 37-47. doi: https://doi.org/https://doi.org/10.1016/0924-2716(91)90005-G.

Gadrani L, G Lominadze and M Tsitsagi. 2018. F assessment of landuse/landcover (LULC) change of Tbilisi and surrounding area using remote sensing (RS) and GIS. *Annals Agrarian Sci* 16: 163-169. doi: https://doi.org/10.1016/j.aasci.2018.02.005.

Goward SN, Y Xue and KP Czajkowski. 2002. Evaluating land surface moisture conditions from the remotely sensed temperature/vegetation index measurements: An exploration with the simplified simple biosphere model. *Remote Sens Environ* 79: 225-242. doi: https://doi.org/https://doi.org/10.1016/S0034-4257(01)00275-9

Guha S and H Govil. 2020. An assessment on the relationship between land surface temperature and normalized difference vegetation index. *Environ Dev Sustain* 23: 1944-1963. doi: https://doi.org/10.1007/s10668-020-00657-6

Huete AR. 1988. A soil-adjusted vegetation index (SAVI). *Remote Sens Environ* 25: 295-309. doi: https://doi.org/https://doi.org/10.1016/0034-4257(88)90106-X.

Ilcheva I and A Yordanova. 2019. Water resource balance for Vitosha Nature Park and adaptive management under conditions of climate change. *Eur J Geography* 10: 56-72.

Kalisa W, T Igbawua, M Henchiri, S Ali, S Zhang, Y Bai and J Zhang. 2019. Assessment of climate impact on vegetation dynamics over East Africa from 1982 to 2015. *Sci Rep* 9: 16865. doi: https://doi.org/10.1038/s41598-019-53150-0.

Khandelwal S, R Goyal, N Kaul and A Mathew. 2018. Assessment of land surface temperature variation due to change in elevation of area surrounding Jaipur, India. *Egypt J Remote Sensing Space Sci* 21: 87-94. doi: https://doi.org/10.1016/j.ejrs.2017.01.005

Nwaerema P, ON Vincent, C Amadou and AI Morrison. 2019. Spatial assessment of land surface temperature and emissivity in the Tropical Littoral City of Port Harcourt, Nigeria. *Int J Environ Climate Change* 9: 88-103. doi: https://doi.org/10.9734/ijecc/2019/v9i230099.

Oliveira S, H Andrade and T Vaz. 2011. The cooling effect of green spaces as a contribution to the mitigation of urban heat: A case study in Lisbon. *Build Environ* 46: 2186-2194. doi: https://doi.org/10.1016/j.buildenv.2011.04.034.

Pal S and S Ziaul. 2017. Detection of land use and land cover change and land surface temperature in English Bazar urban center. *Egypt J Remote Sensing Space Sci* 20: 125-145. doi: https://doi.org/10.1016/j.ejrs.2016.11.003

Rahimzadegan M and AS Janani. 2019. Estimating evapotranspiration of pistachio crop based on SEBAL algorithm using Landsat 8 satellite imagery. *Agr Water Manage* 217: 383-390. doi: https://doi.org/10.1016/j.agwat.2019.03.018

Song L, S Liu, WP Kustas, J Zhou, Z Xu, T Xia and M Li. 2016. Application of remote sensing-based two-source energy balance model for mapping field surface fluxes with composite and component surface temperatures. *Agr Forest Meteorol* 230-231: 8–19. https://doi.org/10.1016/j.agrformet.2016.01.005.

Song R, J-P Muller, S Kharbouche and W Woodgate. 2019. Intercomparison of Surface Albedo Retrievals from MISR, MODIS, CGLS Using Tower and Upscaled Tower Measurements. *Remote Sensing* 11: 644. doi: https://doi.org/10.3390/rs11060644.

Sumunar DRS, N Arif, BS Hadi and K Endro. 2020. Urban energy modeling using remote sensing approaches. *Int J GEOMATE* 19: 203-208. doi: https://doi.org/10.21660/2020.75.23161.

Timmermans WJ, WP Kustas, MC Anderson and AN French. 2007. An intercomparison of the surface energy balance algorithm for land (SEBAL) and the two-source energy balance (TSEB) modeling schemes. *Remote Sens Environt* 108: 369-384. doi: https://doi.org/10.1016/j.rse.2006.11.028

Tursilowati L, J Tetuko, S Sumantyo, H Kuze and ES Adiningsih. 2012. Surface Energy Balance Method into Remote Sensing Application and GIS for Drought Monitoring in Bandung , Indonesia Corresponding Author/ : Laras Tursilowati. *J Emerging Trends in Engineering and Applied Sci* 3: 394-400.

Voogt JA and TR Oke. 2003. Thermal remote sensing of urban climates. *Remote Sens Environ* 86: 370-384. doi: https://doi.org/10.1016/S0034-4257(03)00079-8.

Weng Q. 2009. Thermal infrared remote sensing for urban climate and environmental studies: Methods, applications, and trends. *ISPRS J Photogramm* 64: 335-344. doi: https://doi.org/10.1016/j.isprsjprs.2009.03.007.

Weng Q and D Lu. 2008. A sub-pixel analysis of urbanization effect on land surface temperature and its interplay with impervious surface and vegetation coverage in Indianapolis, United States. *Int J Appl Earth Obs* 10: 68-83. doi: https://doi.org/10.1016/j.jag.2007.05.002.

Zhou W, F Cao and G Wang. 2019. Effects of spatial pattern of forest vegetation on urban cooling in a compact megacity. *Forests* 10: 17-20. doi: https://doi.org/10.3390/f10030282

Zinzi M and E Carnielo. 2017. Impact of urban temperatures on energy performance and thermal comfort in residential buildings. The case of Rome, Italy. *Energy Buildings* 157: 20-29. doi: https://doi.org/10.1016/j.enbuild.2017.05.021